Biosensors and Bioelectronics 193 (2021) 113533

Contents lists available at ScienceDirect

Biosensors and Bioelectronics

journal homepage: www.elsevier.com/locate/bios

Tracking cell migration by cellular force footprint recorded with a mechano-optical biosensor

Ying Tu [a], Xuefeng Wang [a,b,*]

[a] Department of Physics and Astronomy, Iowa State University, Ames, IA, 50011, USA
[b] Molecular, Cellular, and Development Biology Interdepartmental Program, Iowa State University, Ames, IA, 50011, USA

ARTICLE INFO

Keywords:
Cell migration
Cell footprint
Cell adhesive force
Mechano-optical biosensor
Time-lapse microscope

ABSTRACT

Conventional cell migration assays require time-lapse imaging of live cells to trace cell migration paths, consequently demanding cumbersome hardware setup and suffering from low data throughput. In this work, we developed an assay named Tracking Cells by Footprint (TCF) based on a mechano-optical biosensor that irreversibly becomes fluorescent when sensing local cell adhesive force. Cell migration paths are visualized and recorded as fluorescent footprints on glass or elastic substrates coated with such biosensor. From the footprints, cell migration ranges, speeds and persistence are analyzed and quantified without the need of time-lapse imaging. The feasibility of TCF assays was demonstrated with three types of cells with different migratory capabilities. TCF was then applied to evaluating cell motility affected by biochemical or biomechanical cues. The results show that fibroblast motility is reduced by blebbistatin and vinblastine but promoted by bFGF (basic fibroblast growth factor), and the motility correlates with the substrate rigidity. TCF is also compatible with 96-well plates which, combined with static imaging and large-area scanning, provides high data throughput with minimal additional effort.

1. Introduction

Cell migration is an essential process throughout life from embryonic development to apoptosis (Vicente-Manzanares et al., 2005). It is crucial for neutrophils to directionally arrive at the infected region (Horwitz and Webb, 2003; Ridley et al., 2003) and for endothelial cells to relocate towards injury sites during wound healing (Luster et al., 2005; Thomsen et al., 2003). It also plays a significant role in embryogenesis (Hoffman et al., 2011; Lansdown et al., 2001; Poujade et al., 2007; Schwartz, 2010), tumor metastasis (Discher et al., 2005) and more (Joyce and Pollard, 2009; Weijer, 2009). Life-threatening consequences can be caused by mis-regulated cell migration. For example, disabled vascular smooth muscle cell migration results in the failure of vascular development (Lamalice et al., 2007). Abnormal neuron migration can cause developmental disorders in infants (McManus and Golden, 2005) and cancer metastasis has been considered as the dire consequence of upregulated tumor cell migration (Yamaguchi et al., 2005). Because of its pivotal role in many physiological and pathological processes, cell migration has been broadly studied with the quantification of its speed and persistence.

To study cell migration, time-lapse imaging is typically performed to continuously monitor the cell locations within the time window of an experiment (Yilmaz and Christofori, 2010). Fluorescent biosensors have also been applied to track cell locations or to monitor intracellular proteins or signals (Gulyani et al., 2011; Mukherjee et al., 2020). However, live cell migration assay with time-lapse imaging faces two major challenges. First, it imposes a heavy technical demand on the hardware setup. Continuous imaging of live cells requires the integration of a microscope and a cell incubator that keeps cells healthy with controlled temperature, humidity and CO_2 level. Such a setup can be expensive and cumbersome. Moreover, some common technical issues such as stage drifting and imaging defocusing may occur during long-term time-lapse imaging, especially due to unevenly heated microscope components (including the stage and lenses) with local thermal expansion. These issues add uncertainties to the assays and can ruin a painstakingly prepared test. Second, the data throughput of live-cell imaging is limited. High data throughput is often desired for the study of cell migration under many different conditions in parallel, or simply for improving statistical power of a study. For example, in pharmaceutical development, a large library of chemicals (Hughes et al., 2011) are screened to find the promising drugs that may inhibit or upregulate cell migration. Hundreds of chemicals at different concentrations are

* Corresponding author. Department of Physics and Astronomy, Iowa State University, Ames, IA, 50011, USA.
E-mail address: xuefeng@iastate.edu (X. Wang).

https://doi.org/10.1016/j.bios.2021.113533
Received 26 April 2021; Received in revised form 21 June 2021; Accepted 23 July 2021
Available online 27 July 2021
0956-5663/© 2021 Elsevier B.V. All rights reserved.

applied to cells incubated in 96-well plates or 384-well plates. Monitoring cell migratory behaviors in these many samples is problematic if using conventional cell migration assays which typically only monitor cells in one field view for the need of continuous imaging. Although automated stage allows imaging in multiple fields of view, the constant switching of fields of view during each frame of imaging can easily cause large stage drift, and the time interval between two imaging frames may not allow going over a large number of fields of view either. The accumulated data amount could also be staggering. Overall, time-lapse live cell imaging requires a cumbersome hardware setup and has intrinsic difficulty in producing data in high throughput.

To address above two challenges, we developed TCF (Track Cells by Footprint) to record cell migration tracks as cellular force fluorescent footprints. In a typical TCF assay, cell culture surfaces (typically glass surfaces for the good imaging quality) are homogeneously coated with a mechano-optical biosensor, which is initially dark but can be activated to fluoresce by integrin-transmitted cell adhesive force (Wang et al., 2018). Integrins are the main adhesive proteins on the cell membrane mediating cell adhesion and migration (Huttenlocher and Horwitz, 2011; Hynes, 2002). As cells adhere and migrate, integrin-transmitted cellular force activates local biosensor coating and leaves fluorescent marks on the originally dark surfaces. The fluorescence activation is irreversible and activated regions stay fluorescent even after cells move away or are chemically fixed, therefore preserving the whole cell migration tracks. In a TCF assay, cell samples are cultured in an incubator for a desired experiment time (from hours to 1–2 days). After incubation, cell samples are transferred to a fluorescence microscope for the imaging. Because cell incubation and imaging are decoupled in TCF assays, the integration of an incubator and a microscope becomes unnecessary, hence reducing the hardware requirement. The cell samples can be optionally fixed to synchronize cell migration times in all tested conditions (as cell imaging takes time). Information of cell migration range, speed and persistence is extracted from the cell footprints in the static photos. This allows large-area scanning in one sample or imaging many samples with reasonable effort, therefore substantially increasing data throughput.

The mechano-optical biosensor used in this assay is integrative tension sensor (ITS) previously developed in our lab (Wang and Ha, 2013; Wang et al., 2018). Briefly, ITS is a double-stranded DNA or a DNA/PNA (peptide nucleic acid) hybrid duplex labeled with a pair of quencher and fluorophore and equipped with a RGD (arginylglycylaspartic acid) peptide ligand (Pierschbacher and Ruoslahti, 1984) targeting integrin. The DNA/PNA duplex is preferred for long-term cell incubation for its better resistance to the degradation caused by DNase secreted by cells during cell culture (Zhao et al., 2020b). Immobilized on a surface, the ITS becomes fluorescent when the dsDNA or the DNA/PNA duplex is mechanically disassociated by the force transmitted by integrin-RGD ligand bonds. Previously, ITS was mainly used to study cell adhesive force and force-structure interplay in adherent cells. Here, ITS is adopted to record cell migration tracks in the TCF assay.

2. Materials and methods

2.1. Preparation of ITS

ITS was synthesized by hybridizing a DNA upper strand and a PNA lower strand. The DNA strand is labeled with a blackhole quencher (BHQ_2) and a RGD peptide, and the PNA strand is labeled with a fluorophore and a biotin (Fig. 1B). DNA was customized and purchased from Integrated DNA Technologies. PNA was customized and purchased from PNA Bio Inc. The ligand, a cyclic arginine-glycine-aspartic acid peptide (RGD), was conjugated to the DNA strand using thiol modification. The RGD-DNA conjugation protocol is detailed in these articles (Zhao et al. 2019, 2020b). Briefly, cyclic peptide RGD with an amine group (PCI-3696-PI, Peptides International) was conjugated with the DNA strand with thiol modification. The thiol modification on 5' end of DNA was deprotected by TCEP (Tris(2-carboxyethyl)phosphine hydrochloride) and reacted with the maleimide group of a heterolinker SMCC-sulfo (22622, thermos scientific). The other end of SMCC-sulfo is an NHS ester (N-hydroxysuccinimide esters) which reacts with the amine of RGD. The RGD conjugated DNA was purified by electrophoresis.

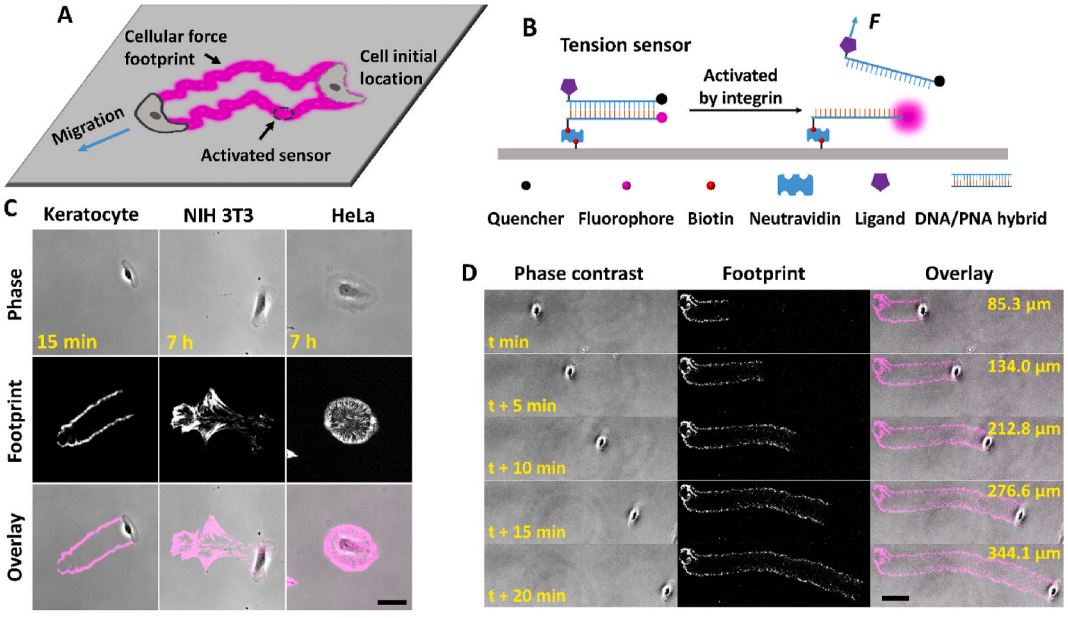

Fig. 1. Reporting cell migration paths by cell footprint recorded by mechano-optical biosensor. (**A**) The principle of the TCF (Track Cells by Footprint) assay. A cell leaves 'footprint' by activating tension sensor (ITS), a mechano-optical biosensor, to fluoresce along the migration path. (**B**) ITS consists of a DNA/PNA hybrid decorated with a pair of quencher and fluorophore and a ligand (RGD). If the PNA/DNA hybrid is ruptured by the cellular force transmitted by integrins, the originally quenched fluorophore becomes fluorescent. (**C**) Footprints of fast migrating cells (keratocytes, 15 min), slow migrating cells (NIH 3T3 fibroblasts, 7 h) and static cells (HeLa, 7 h) on the TCF platform. (**D**) Time-series images of keratocyte footprint developed in 20 min. The cell migrated for 48.7, 127.5, 191.3, and 258.8 μm in 5, 10, 15 and 20 min, respectively. Scale bars: 50 μm.

The sequences and modifications of the DNA and PNA strands are:

DNA upper strand: 5'-/RGD/GGG CGG CGA CCT CAG CAT/BHQ_2/-3'.

PNA lower strand: 5′-Cy5-O- ATG CTG AGG TCG CCG CCC -KKK (Biotin).where the BHQ_2 and Cy5 are the black hole quencher and the fluorophore, and "-O-" linker (2-aminoethoxy-2-ethoxy acetic acid) and K (lysine) are inserted to increase PNA solubility in water or in PBS (phosphate-buffered saline). BHQ_2 and Cy3 are also a good quencher-dye pair if the optical spectrum of Cy3 is desired in fluorescence imaging.

Alternatively, DNA lower strand: 5'-/Cy5/ATG CTG AGG TCG CCG CCC/Biotin/-3′ can be used instead of the PNA strand if the TCF assay time is short (e.g., 2–3 h) and DNase activity is low in the cell culture medium.

The ITS was assembled by hybridizing the upper strand and the lower strand with a concentration ratio of 1.1:1.

2.2. ITS surface coating

During assays, ITS was immobilized on a glass bottom petri-dish (D35-14-1.5-N, Cellvis) or a glass bottom 96-well plate (P96-1-N, Cellvis). The glass surfaces were firstly coated with 100 μg/mL biotinylated bovine serum albumin (BSA-biotin, Sigma-Aldrich, A8549) spiked with 5 μg/mL fibronectin (R&D Systems, 1918-FN) that facilitates cell normal adhesion and migration. After 20-min incubation, the surfaces were washed with PBS (phosphate buffered saline) three times. Next, the surfaces were incubated with 50 μg/mL neutravidin (Thermo Scientific, 31000) for 20 min and washed with PBS. At last, the surfaces were incubated with 50 nM (nano-Molar) ITS for 20 min and washed with PBS. ITS coating procedure on PDMS gels is the same as that on glass surfaces because PDMS gels, like glass surfaces, have strong physical adsorption to BSA-biotin.

2.3. Cell culture and plating

Fast migrating cells, keratocytes were harvested from a goldfish (carassius auratus). A fish scale was gently plucked and pressed onto a petri-dish. After 1 min allowing the scale to adhere onto the surface, 2 mL culture medium (79 % IMDM + 20 % fetal bovine serum + 1 % penicillin/streptomycin) was added to the petri-dish and the sample was placed in a sterilized box (or other small-sized containers) at room temperature overnight. The keratocytes migrated out from the fish scale and were ready to use. NIH 3T3 cells and HeLa cells were purchased from ATCC (American Type Culture Collection) and cultured according to the culture methods in ATCC.org. Stationary cells (HeLa cells) and slow migrating cells (NIH 3T3 cells) were harvested after culturing for 3 days or when the cell confluency was higher than 90 %. To plate cells on ITS surfaces, the cells were detached from culture flasks using 2 mL mild detaching solution (recipe: 100 mL of 10 × HBSS, 10 mL of 1 M HEPES, 10 mL of 7.5 % sodium bicarbonate, 2.4 mL of 500 mM EDTA and 878 mL H_2O with final pH 7.6) with 5–10 min treatment time. The detached cells were dispersed, collected and centrifuged for 3 min at 300 RCF. The cell pellets were re-suspended with culture medium to obtain a final cell density of around 1×10^5/mL. We used a relatively low cell density to allow enough area for cells to migrate. The cell solution was plated onto ITS surfaces which were incubated in an incubator supplied with 5 % CO_2 and at 37 °C. The incubation duration was set to be 3 h, 5 h, 7 h, or 24 h to study the cell migration. Keratocytes were not centrifuged and were incubated at room temperature without extra CO_2 supply for 30 min, 50 min, 70 min and 120 min. Keratocytes live well at room temperature as fish are cold-blooded animals. After incubation, all testing cells were fixed with 4 % formaldehyde (Thermo Scientific, 31000, 28906) for 15 min at room temperature, rinsed with PBS three times and imaged by a Nikon-E fluorescence microscope.

2.4. Preparation of PDMS substrates

Polydimethylsiloxane (PDMS) gels were prepared by mixing elastomer base and crosslinker (04019862, SYLGARD 184 silicone elastomer kit). The base and crosslinker were mixed thoroughly in ratios 30:1 and 50:1, resulting in rigidity of 213 kPa and 12 kPa calibrated by atomic force microscopy, respectively. A 5 μL droplet of each mixture was sandwiched between two glass coverslips and kept for 15 min before separation. The two coverslips coated with PDMS mixture were kept to rest for 30 min so that the PDMS coating becomes uniform on the surfaces. Next, the coverslips were cured at 70 °C overnight on a hotplate. The coverslips were then removed from the hotplate and cooled down slowly. The ready-for-use PDMS coverslip was mounted onto an empty-bottom petri-dish (D35-14, Cellvis) by an UV light-activated glue. The process of ITS immobilization on these surfaces was identical to that on regular glass surfaces.

2.5. Drug treatments

Drug treatments were performed during cell plating. After the cell pellets were re-suspended with culture medium, the cell suspension was mixed with medium containing blebbistatin (B0560, Sigma), vinblastine (V1377, Sigma) or basic fibroblast growth factor (450-33, Pepro Tech), respectively.

2.6. Recording cell migration 'footprint'

Fluorescence and phase contrast imaging of cells were conducted with an epi-fluorescence microscope (Ti-E, Nikon) with a 20 × lens (Plan Fluor 20 × /N.A. 0.75, Nikon). Large-area scan was achieved by imaging and stitching n × n adjacent fields of view (n is an integer). Cell migration distances were calculated by measuring the contour length of the cell footprints with ImageJ (1.52a).

3. Results and discussions

3.1. Recording cell migration paths as fluorescent footprint on the TCF platform

Many metazoan cell adhesion and migration are mediated by membrane protein integrins. The common types of integrins such as integrin $\alpha_{IIb}\beta_3$, $\alpha_V\beta_3$ and $\alpha_5\beta_1$ bind to a peptide RGD motif found in ligand proteins including fibronectin, vitronectin and Von Willebrand factor (Humphries et al., 2006). Cells constantly generate traction force on the integrin-ligand bonds during cell adhesion and migration. On the TCF platform, integrin tension sensor (ITS) as a mechano-optical biosensor is immobilized on glass surfaces of a glass-bottomed petri-dish or 96-well plates to record the cell-substrate mechanical interaction by fluorescence. Fig. 1A illustrates a migrating cell producing fluorescent footprint by switching on ITS, demonstrating the principle of the TCF assay in reporting cell migration paths. ITS is initially dark due to the quenching effect until being activated by integrin-ligand-transmitted cellular force, which mechanically dissociates the dsDNA or the DNA/PNA hybrid duplex in the ITS, hence freeing the fluorophore (Cy5 in our work) on the lower strand from quenching (Fig. 1B). The DNA/PNA hybrid in the ITS is in unzipping configuration that can be readily opened by integrin tensions (Zhao et al., 2020b). The DNA/PNA hybrid was adopted to resist the potential sensor degradation caused by DNase from cells. To minimize the impact of ITS rupture to cell adhesion and migration, the surface was also co-coated with fibronectin that provides non-rupturable integrin ligands ensuring cell normal adhesion and migration. In Fig. 1C, three types of cells with different migrating capacities were plated on ITS surfaces and cultured for 15 min for fish keratocytes (fast migrating cells), 7 h for NIH 3T3 fibroblasts (slow migrating cells) and 7 h for HeLa cells (stationary cells), respectively. The ITS surfaces successfully recorded force footprints for all the cells.

The keratocyte produced a footprint of ~141 μm length during 15 min incubation, the NIH 3T3 cell generated a footprint of ~150 μm length in 7 h, and the HeLa cell produced a force pattern co-localized with the cell body, suggesting little motility of the HeLa cell.

To verify that the force footprint indeed reports cell migration tracks, we monitored the development of cell footprint in real-time with time-lapse microscopy. As shown in Fig. 1D, a migrating keratocyte was continuously imaged on an ITS surface for 20 min. The cell body reported by the phase-contrast imaging was consistently located at the front end of the footprint, demonstrating that the force footprint reports the cell migration track properly. The cell migration ranges reported by the fluorescent force tracks are 48.7 μm for the first 5 min and 258.8 μm for 20 min.

3.2. Low hardware demand and high data throughput of TCF assays

Conventional cell migration assay requires continuous imaging of live cells with a time-lapse microscope integrated with supplies of CO_2, temperature and humidity at proper levels. Researchers also need to address technical challenges such as stage drift, image defocusing, cell phototoxicity and limited imaging field of view (cells might migrate out of field of view) which commonly emerge in long-term live cell imaging. Moreover, the data throughput is low, as long-term live cell imaging usually only monitors cells under one testing condition, making those assays requiring high data throughput, such as screening chemicals affecting cell migration, extremely time-consuming and cost-ineffective. In contrast, TCF assay captures cell migration tracks in static photos. Cell incubation and imaging are decoupled, allowing cell incubation in a cell incubator and cell footprint imaging with a regular microscope afterwards. Therefore, the TCF assay has modest hardware requirement for cell incubation and imaging.

We also confirmed that the TCF assay can be performed with glass-bottom 96-well plates (Fig. 2A), the standard apparatus used in drug screening. This compatibility allows testing cell migration in numerous biochemical conditions in parallel. Cells can be fixed after incubation and prior to cell imaging to synchronize the migration time. Cell fixation with ethanol or paraformaldehyde does not damage the cell footprints on the surface according to our test. Because the migration tracks are recorded in single static images, large-area scan can be performed on the cell-culturing surface to obtain many cell migration tracks in one sample. Large-area scan is an imaging feature commonly installed in a microscope equipped with an automated stage that enables imaging and stitching of multiple fields of view to one photo covering a large area. Fig. 2B and C are examples showing migration tracks of NIH 3T3 and HeLa cells in large-area scans.

Overall, with the decoupling of cell incubation and cell imaging, compatibility with 96-well plates, cell fixation and large-area scan, TCF assays substantially reduce the hardware demand and increase data throughput in cell migration assays.

3.3. Quantifying cell migration ranges and speeds with TCF assays

Cell migration ability varies (Wang and Ha, 2013; Zhao et al., 2020a) and is often evaluated with three factors: range, speed and persistence. Here we show that these factors can be quantified with the force footprints. We performed TCF assays with keratocytes, NIH 3T3 and HeLa cells with different incubation times. Four keratocyte samples were plated and incubated on ITS surfaces for 30, 50, 70 and 120 min, respectively. The migration ranges were quantified by measuring the contour lengths of the footprints (Fig. 3A and D). The average speed of keratocyte migration was calculated to be 404.3 μm/h (Fig. 3G) in 2 h. In a similar procedure, four NIH 3T3 cell samples were incubated on ITS surfaces for 3, 5, 7 and 24 h, respectively, and the migration ranges were quantified accordingly (Fig. 3B and E). The average migration speed is 10.2 μm/h in 24 h, about 2.5 % of keratocyte migration speed. Four HeLa cell samples were also tested with incubation times of 3, 5, 7 and 24 h, respectively (Fig. 3C and F). The average migration speed was 2.5 μm/h in 24 h, much lower than that of NIH 3T3 cells. Fig. 3G shows the average migration speeds of three cell types in different periods. t1-t4 represent 30, 50, 70 and 120 min for keratocytes, and 3, 5, 7 and 24 h for NIH 3T3 and HeLa cells. The migration ranges and speeds of the three cell types are summarized in Table 1.

3.4. Quantifying cell migration persistence with TCF assays

Cell migration persistence can also be evaluated by analyzing the

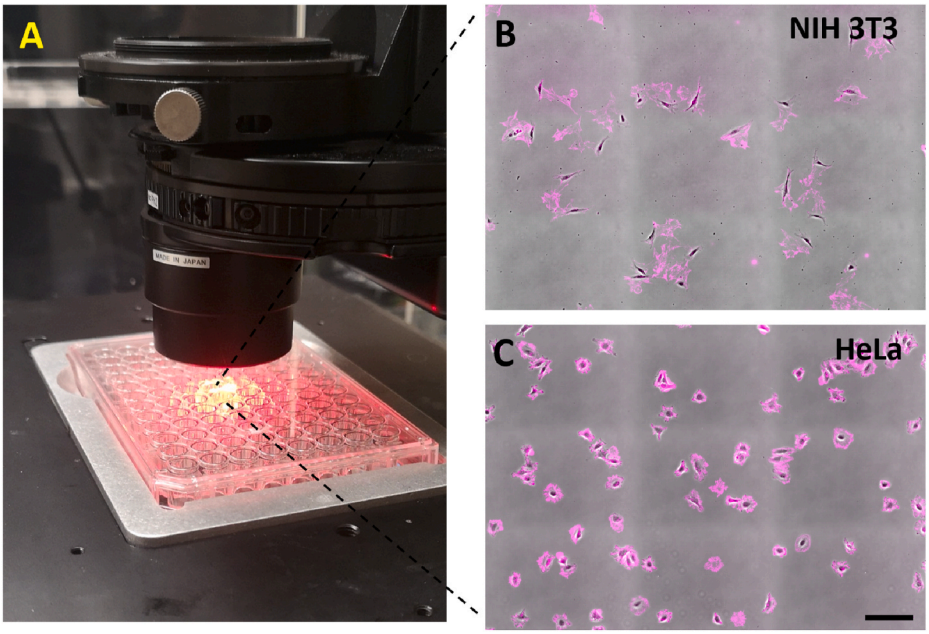

Fig. 2. The TCF assay is compatible with 96-well plates, cell fixation and large-area scan. (**A**) NIH 3T3 fibroblasts and HeLa cells were cultured in a 96-well plate coated with ITS. (**B, C**) Large-area scan (only 3 × 3 adjacent fields shown here for image clarity) shows migration tracks (footprints) of many individual cells. Scale bar: 200 μm.

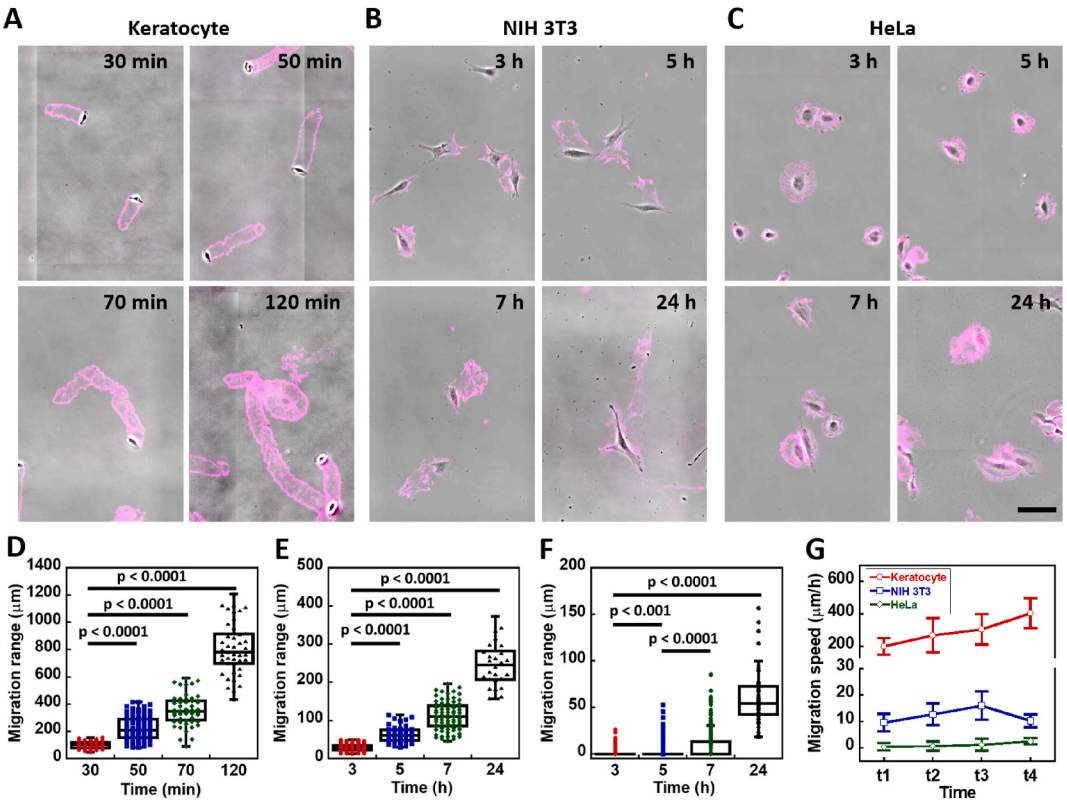

Fig. 3. Analysis of cell migration ranges and speeds on TCF platforms. (**A-C**) Cellular force footprints of keratocytes, NIH 3T3 cells and HeLa cells at different incubation times. (**D**) Migration ranges of keratocytes. (**E**) Migration ranges of NIH 3T3 cells. (**F**) Migration ranges of HeLa cells. (**G**) Average migration speeds of three cell types with different incubation times. t1-t4 are 30, 50, 70 and 120 min for keratocyte, and 3, 5, 7 and 24 h for NIH 3T3 and HeLa. Error bars represent standard deviations. 50–200 cells were analyzed for each data point. Scale bar: 100 μm.

Table 1
A summary of cell migration range and speed.

		Migration range (μm)	Migration speed (μm/h)
Keratocyte	30 min	99.9 ± 25.6	199.8 ± 51.2
	50 min	223.4 ± 88.1	268.1 ± 105.7
	70 min	354.9 ± 108.8	304.2 ± 93.3
	120 min	808.5 ± 186.9	404.3 ± 93.5
NIH 3T3	3 h	28.8 ± 9.8	9.6 ± 3.3
	5 h	63.5 ± 20.5	12.7 ± 4.1
	7 h	111.8 ± 37.1	16.0 ± 5.3
	24 h	244.9 ± 57.5	10.2 ± 2.4
HeLa	3 h	1.25 ± 4.15	0.4 ± 1.4
	5 h	3.34 ± 8.8	0.7 ± 1.8
	7 h	8.3 ± 16.1	1.2 ± 2.3
	24 h	60.4 ± 28	2.5 ± 1.2

cellular force footprints. Migration persistence is important for a cell maintaining a direction and arriving at a targeted location (Dunn, 1983). Directionality ratio, one relatively simple and intuitive factor, is often used to evaluate the persistence of cell migration (Gorelik and Gautreau, 2014). The directionality ratio is defined as the quotient of the start-to-end distance (D) of a migration track and the track contour length (L) (Fig. 4A). A straight cell migration track results in a directionality ratio of 1, and lower ratio indicates lower migration persistence. Note that directionality ratio is not a constant intrinsic to a cell type, but depends on the overall cell migration time and range (longer migration time or range usually reduces this ratio). Other factors independent of migration time, e.g., the average direction change in angle per unit migration length (Gorelik and Gautreau, 2014), have been proposed to describe cell migration persistence. Such factors can also be extracted by analyzing cellular force footprints as well. Here we only analyzed directionality ratio for demonstration for its simplicity. For the comparison of directionality ratios across different cell types, we compared them on the basis of similar migration contour lengths.

In Fig. 4A–B, the contour lengths of a NIH 3T3 fibroblast and a keratocyte are 248.0 μm and 266.8 μm, respectively. The distances between the start point and endpoint are 173.5 μm for the NIH 3T3 cell and 246.7 μm for the keratocyte, resulting in directionality ratio 0.7 for NIH 3T3 cells and 0.92 for keratocytes (Fig. 4C). This demonstrates that NIH 3T3 cells assumed a more meandering migration pattern compared to keratocytes. When the contour length became longer, the directionality ratio of keratocytes also decreased (Fig. 4D), especially at 50–70 min incubation time. Overall, the TCF platform is adequate and convenient for evaluating cell migration persistence.

3.5. *Evaluating the effect of biochemical treatments on cell migration with TCF assays*

Next, we tested the capability of TCF platform in evaluating drug effects on cell migration. NIH 3T3 cells were cultured with blebbistatin, vinblastine and basic fibroblast growth factor (bFGF), respectively, and incubated for 7 h on the TCF platforms. Blebbistatin is a myosin II inhibitor that reduces cell contraction and may interfere cell migration (Huber et al., 2013). Vinblastine is a microtubule-disruptive reagent used in cancer chemotherapy. Previous research reported that vinblastine may reduce cell motility (Yang et al., 2010). bFGF is a cytokine that stimulates cell growth and reportedly promotes cell motility (Jackson and Reidy, 1993; Rifkin and Moscatelli, 1989). In Fig. 5A, migration speeds of the cells treated with blebbistatin were significantly suppressed. The migration speed decreased from 15.7 μm/h (control) to 8.8 μm/h in 1 μM blebbistatin and further to 7.5 μm/h in 5 μM blebbistatin (Fig. 5D). In another test, NIH 3T3 cells were treated with vinblastine at various concentrations and plated on the TCF platform for 7 h. The cell

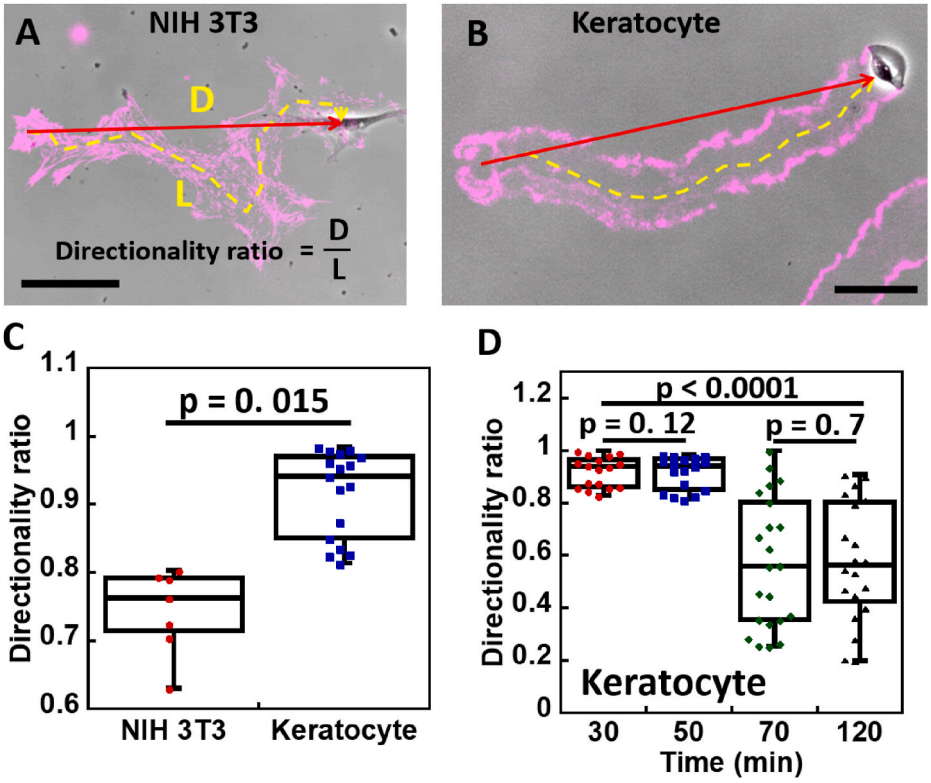

Fig. 4. Migration persistence analysis. (**A**) An NIH 3T3 cell cultured on the TCF platform for 24 h. D is the distance between the start point to the endpoint of the migration track (footprint). L is the contour length of the track. Directionality ratio = D/L. (**B**) A keratocyte cell cultured for 50 min. (**C**) Directionality ratios of NIH 3T3 cells and keratocytes compared at similar migration contour lengths of ~250 μm. (**D**) Directionality ratio of keratocyte migration versus time. 10–50 cells were analyzed for each data point. Scale bars: 50 μm.

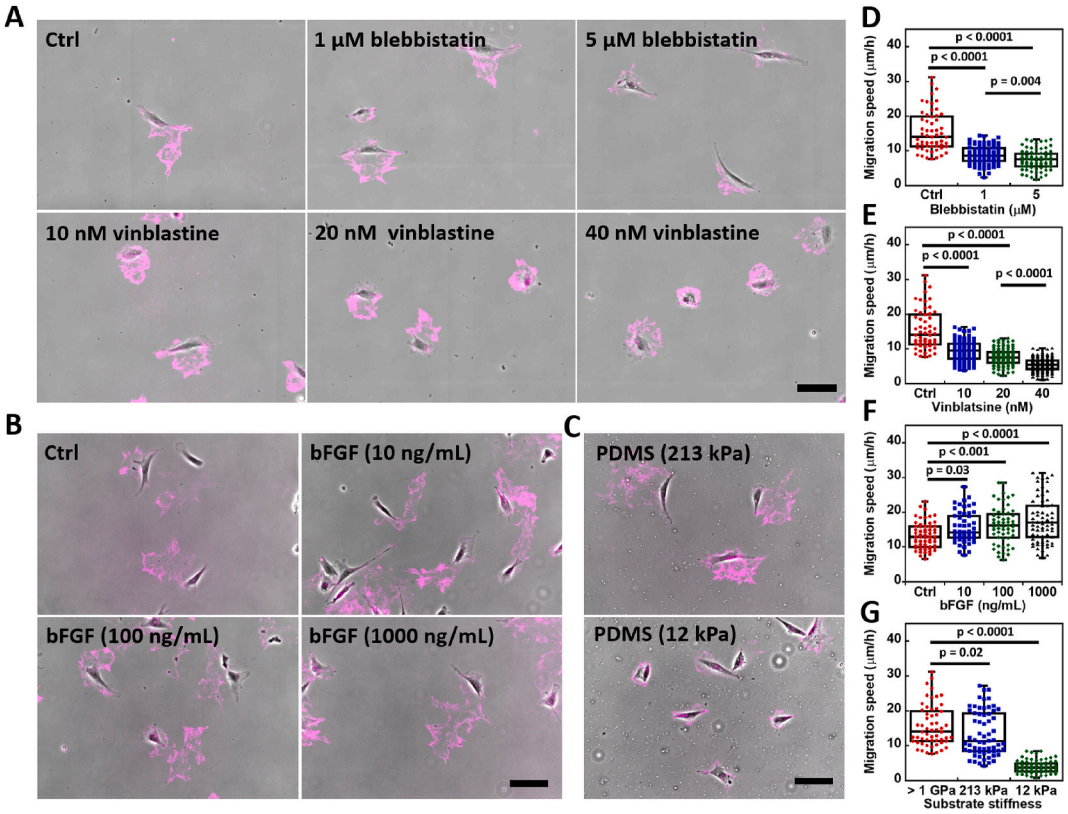

Fig. 5. Cell migration affected by biochemical and biomechanical cues. (**A**) Migration footprints of NIH 3T3 treated with blebbistatin (1 μM, 5 μM) or vinblastine (10 nM, 20 nM, 40 nM). (**B**) Migration footprints of NIH 3T3 cells treated with basic fibroblast factor (bFGF, 10 ng/mL, 100 ng/mL, 1000 ng/mL). (**C**) Migration footprints of NIH 3T3 cells on PDMS substrates (213 kPa, 12 kPa). (**D**) The average migration speeds of NIH 3T3 cells treated with blebbistatin. (**E**) The average migration speeds of NIH 3T3 cells treated with vinblastine. (**F**) The average migration speeds of NIH 3T3 cells treated with bFGF. (**G**) NIH 3T3 cells migration speeds versus substrate elasticities. 50–200 cells were analyzed for each data point. Scale bars: 100 μm.

migration ranges and speeds were remarkably suppressed with vinblastine treatments (Fig. 5A and E). Cell migration speed decreased from 15.7 μm/h (control) to 9.4 μm/h in 10 nM vinblastine and further to 7.7 μm/h and 5.5 μm/h with 20 nM and 40 nM vinblastine, respectively (Fig. 5E). Because vinblastine disrupts microtubule assembly (Panda et al., 1996) which is critically important for many basic cell functions including cell migration (Etienne-Manneville, 2013), we are not certain that the inhibitory effect of vinblastine on cell migration is specific or an indirect consequence due to the general cell health damage. In Fig. 5B, NIH 3T3 cells were cultured with bFGF of different concentrations for 7 h, the migration tracks show slight increments as bFGF concentration increases. The cell migration speed was increased from 13.3 μm/h (control) to 15.5 μm/h in 10 ng/mL bFGF and further to 16.3 μm/h and 17.6 μm/h in 100 ng/mL and 1000 ng/mL bFGF, respectively (Fig. 5F). Although the mechanism of how bFGF promotes NIH 3T3 cell migration is not fully clear, the TCF platform has been shown to be applicable for screening drugs that promote or demote cell migration.

3.6. *Evaluating the effect of biomechanical cues on cell migration with TCF assays*

The TCF assays were also applied to reporting cell migration on elastic substrates. Polydimethylsiloxane (PDMS) gel layers on glass were prepared at two elastic moduli (213 kPa, 12 kPa) by adjusting the volume ratio of base and crosslinker (Trappmann et al., 2012). NIH 3T3 cells were plated and cultured for 7 h on glass (>1 GPa) and PDMS substrates coated with ITS. The procedure of ITS coating on PDMS surfaces is identical to that on glass surfaces. In Fig. 5C, cells generated fluorescent migration tracks on the PDMS surfaces, indicating that the TCF platform is compatible with elastic substrates. Analysis of migration tracks on the glass (Fig. 5A) and two PDMS surfaces (Fig. 5C) shows that cell motility was slightly reduced on 213 kPa PDMS (13.4 μm/h) but markedly suppressed on 12 kPa PDMS surface (4.0 μm/h). Cells retained 85 % of their motility on 213 kPa PDMS gel and only 25 % on a softer (12 kPa) surface (Fig. 5G). The result demonstrates that migration speed of NIH 3T3 fibroblasts is correlated with the substrate rigidity, suggesting that cell migration is a rigidity-dependent behavior and the migration ability is weakened on substrates with low rigidities. This result of rigidity-dependence is consistent with a previous report (Hartman et al., 2017), demonstrating that TCF assays are applicable in reporting cell migration on elastic substrates.

4. Conclusion

We developed a TCF assay to evaluate cell motility by cellular force footprints recorded on a mechano-optical biosensor ITS. The TCF platform coated with such biosensor converts cell adhesive force to permanent fluorescent mark on a surface, hence recording cell migration tracks as fluorescent footprints. The spatial resolution of force imaging obtained by ITS was previously demonstrated as 0.4 μm (Wang et al., 2018), which is sufficient for tracking the migration of small mammalian cells or cell fragments (such as platelets). The footprints faithfully report cell migration paths, obviating the need of monitoring live cells with time-lapse microscopy which is technically challenging and has low data throughput. We tested TCF assays with three types of cells with high, intermediate and poor migration capabilities, respectively. TCF assays successfully reported cell migration ranges, speeds and persistence. This method is compatible with 96-well plates and suitable for drug screening or other cell migration examinations requiring high data throughput.

Currently, there are other cell migration and invasion assays that are compatible with 96-well plates and able to examine cell migration under numerous conditions in parallel, such as *in vitro* wound healing assay (scratch assay) (Liang et al., 2007), transwell migration assay (Boyden chamber assay), etc (Kramer et al., 2013). However, these assays cannot achieve single cell tracking while retaining the high data throughput, as cell tracking by video recording is time-consuming and usually conflicts with the process of monitoring a large number of samples simultaneously. In summary, TCF assays track cell migration with static imaging, significantly reducing the technical demand of cell migration study and improving data throughput with minimal additional efforts.

Author contributions

X.W. and Y.T. conceived the project and designed the experiments. Y. T. performed experiments and collected data. Y.T. and X.W. analyzed the data. X.W. and Y.T. wrote the manuscript.

CRediT authorship contribution statement

Ying Tu: Methodology, Data curation, Formal analysis, Writing – original draft. **Xuefeng Wang:** Conceptualization, Funding acquisition, Methodology, Writing – review & editing.

Declaration of competing interest

The authors declare that they have no known competing financial interests or personal relationships that could have appeared to influence the work reported in this paper.

Acknowledgement

The work was funded by National Institute of General Medical Sciences (1R35GM128747) and by National Science Foundation (1825724).

References

Discher, D.E., Janmey, P., Wang, Y.L., 2005. Tissue cells feel and respond to the stiffness of their substrate. Science 310 (5751), 1139–1143.
Dunn, G.A., 1983. Characterising a kinesis response: time averaged measures of cell speed and directional persistence. Agents and actions. Supplement 12, 14–33.
Etienne-Manneville, S., 2013. Microtubules in cell migration. Annu. Rev. Cell Dev. Biol. 29, 471–499.
Gorelik, R., Gautreau, A., 2014. Quantitative and unbiased analysis of directional persistence in cell migration. Nat. Protoc. 9 (8), 1931–1943.
Gulyani, A., Vitriol, E., Allen, R., Wu, J., Gremyachinskiy, D., Lewis, S., Dewar, B., Graves, L.M., Kay, B.K., Kuhlman, B., Elston, T., Hahn, K.M., 2011. A biosensor generated via high-throughput screening quantifies cell edge Src dynamics. Nat. Chem. Biol. 7 (7), 437–444.
Hartman, C.D., Isenberg, B.C., Chua, S.G., Wong, J.Y., 2017. Extracellular matrix type modulates cell migration on mechanical gradients. Exp. Cell Res. 359 (2), 361–366.
Hoffman, B.D., Grashoff, C., Schwartz, M.A., 2011. Dynamic molecular processes mediate cellular mechanotransduction. Nature 475 (7356), 316–323.
Horwitz, R., Webb, D., 2003. Cell migration. Curr. Biol. 13 (19), R756–R759.
Huber, F., Schnauß, J., Rönicke, S., Rauch, P., Müller, K., Fütterer, C., Käs, J., 2013. Emergent complexity of the cytoskeleton: from single filaments to tissue. Adv. Phys. 62 (1), 1–112.
Hughes, J.P., Rees, S., Kalindjian, S.B., Philpott, K.L., 2011. Principles of early drug discovery. Br. J. Pharmacol. 162 (6), 1239–1249.
Humphries, J.D., Byron, A., Humphries, M.J., 2006. Integrin ligands at a glance. J. Cell Sci. 119 (19), 3901–3903.
Huttenlocher, A., Horwitz, A.R., 2011. Integrins in cell migration. Csh Perspect. Biol. 3 (9).
Hynes, R.O., 2002. Integrins: bidirectional, allosteric signaling machines. Cell 110 (6), 673–687.
Jackson, C.L., Reidy, M.A., 1993. Basic fibroblast growth factor: its role in the control of smooth muscle cell migration. Am. J. Pathol. 143 (4), 1024–1031.
Joyce, J.A., Pollard, J.W., 2009. Microenvironmental regulation of metastasis. Nat. Rev. Canc. 9 (4), 239–252.
Kramer, N., Walzl, A., Unger, C., Rosner, M., Krupitza, G., Hengstschläger, M., Dolznig, H., 2013. In vitro cell migration and invasion assays. Mutat. Res. Rev. Mutat. Res. 752 (1), 10–24.
Lamalice, L., Le Boeuf, F., Huot, J., 2007. Endothelial cell migration during angiogenesis. Circ. Res. 100 (6), 782–794.
Lansdown, A.B.G., Sampson, B., Rowe, A., 2001. Experimental observations in the rat on the influence of cadmium on skin wound repair. Int. J. Exp. Pathol. 82 (1), 35–41.
Liang, C.-C., Park, A.Y., Guan, J.-L., 2007. In vitro scratch assay: a convenient and inexpensive method for analysis of cell migration in vitro. Nat. Protoc. 2 (2), 329–333.
Luster, A.D., Alon, R., von Andrian, U.H., 2005. Immune cell migration in inflammation: present and future therapeutic targets. Nat. Immunol. 6 (12), 1182–1190.

McManus, M.F., Golden, J.A., 2005. Neuronal migration in developmental disorders. J. Child Neurol. 20 (4), 280–286.
Mukherjee, A., Singh, R., Udayan, S., Biswas, S., Reddy, P.P., Manmadhan, S., George, G., Kumar, S., Das, R., Rao, B.M., Gulyani, A., 2020. A Fyn biosensor reveals pulsatile, spatially localized kinase activity and signaling crosstalk in live mammalian cells. Elife 9.
Panda, D., Jordan, M.A., Chu, K.C., Wilson, L., 1996. Differential effects of vinblastine on polymerization and dynamics at opposite microtubule ends. J. Biol. Chem. 271 (47), 29807–29812.
Pierschbacher, M.D., Ruoslahti, E., 1984. Cell attachment activity of fibronectin can Be duplicated by small synthetic fragments of the molecule. Nature 309 (5963), 30–33.
Poujade, M., Grasland-Mongrain, E., Hertzog, A., Jouanneau, J., Chavrier, P., Ladoux, B., Buguin, A., Silberzan, P., 2007. Collective migration of an epithelial monolayer in response to a model wound. Proc. Natl. Acad. Sci. USA 104 (41), 15988–15993.
Ridley, A.J., Schwartz, M.A., Burridge, K., Firtel, R.A., Ginsberg, M.H., Borisy, G., Parsons, J.T., Horwitz, A.R., 2003. Cell migration: integrating signals from front to back. Science 302 (5651), 1704.
Rifkin, D.B., Moscatelli, D., 1989. Recent developments in the cell biology of basic fibroblast growth factor. JCB (J. Cell Biol.) 109 (1), 1–6.
Schwartz, M.A., 2010. Integrins and extracellular matrix in mechanotransduction. Csh Perspect. Biol. 2 (12).
Thomsen, A.R., Nansen, A., Madsen, A.N., Bartholdy, C., Christensen, J.P., 2003. Regulation of T cell migration during viral infection: role of adhesion molecules and chemokines. Immunol. Lett. 85 (2), 119–127.
Trappmann, B., Gautrot, J.E., Connelly, J.T., Strange, D.G.T., Li, Y., Oyen, M.L., Cohen Stuart, M.A., Boehm, H., Li, B., Vogel, V., Spatz, J.P., Watt, F.M., Huck, W.T.S., 2012. Extracellular-matrix tethering regulates stem-cell fate. Nat. Mater. 11 (7), 642–649.
Vicente-Manzanares, M., Webb, D.J., Horwitz, A.R., 2005. Cell migration at a glance. J. Cell Sci. 118 (21), 4917.
Wang, X., Ha, T., 2013. Defining single molecular forces required to activate integrin and notch signaling. Science 340 (6135), 991–994.
Wang, Y., LeVine, D.N., Gannon, M., Zhao, Y., Sarkar, A., Hoch, B., Wang, X., 2018. Force-activatable biosensor enables single platelet force mapping directly by fluorescence imaging. Biosens. Bioelectron. 100, 192–200.
Weijer, C.J., 2009. Collective cell migration in development. J. Cell Sci. 122 (18), 3215–3223.
Yamaguchi, H., Wyckoff, J., Condeelis, J., 2005. Cell migration in tumors. Curr. Opin. Cell Biol. 17 (5), 559–564.
Yang, H.L., Ganguly, A., Cabral, F., 2010. Inhibition of cell migration and cell division correlates with distinct effects of microtubule inhibiting drugs. J. Biol. Chem. 285 (42), 32242–32250.
Yilmaz, M., Christofori, G., 2010. Mechanisms of motility in metastasizing cells. Mol. Canc. Res. 8 (5), 629–642.
Zhao, Y., Pal, K., Tu, Y., Wang, X., 2020a. Cellular force nanoscopy with 50 nm resolution based on integrin molecular tension imaging and localization. J. Am. Chem. Soc. 142 (15), 6930–6934.
Zhao, Y., Sarkar, A., Wang, X., 2020b. Peptide nucleic acid based tension sensor for cellular force imaging with strong DNase resistance. Biosens. Bioelectron. 150, 111959.
Zhao, Y.C., Wetter, N.M., Wang, X.F., 2019. Imaging integrin tension and cellular force at submicron resolution with an integrative tension sensor. Jove-J. Vis. Exp. 146.